Effect of oxygen on the optical properties of small silicon pyramidal clusters

A. B. Filonov
Belarusian State University of Informatics and Radioelectronics, P. Browka 6, 220027 Minsk, Belarus

Stefano Ossicini
Istituto Nazionale della Fisica della Materia (INFM) and Dipartimento di Fisica, Universitá di Modena e Reggio Emilia, Via Campi 213/A, 41100 Modena, Italy

F. Bassani and F. Arnaud d'Avitaya
Centre de Recherche sur les Mécanismes de la Croissance Cristalline, Campus de Luminy, case 913, 13288 Marseille Cedex 9, France
(Received 18 January 2001; published 8 May 2002)

Optical absorption and light emission of oxygen-incorporated small silicon ($Si_{30}H_{40}O_i$) pyramidal clusters as a function of oxygen content were theoretically studied using the self-consistent semiempirical molecular orbital method (modified neglect of diatomic overlap—parametric method 3). In the absolute majority of the cluster configurations with low oxygen content ($i<4$) the excitations have a strong localized character and result in a significant shift from its equilibrium ground state position of one of the silicon atoms inside the cluster volume. The optical transition energies in those cases range from 2.05 to 2.35 eV. The typical Stokes shift for these structures is of the order of 100 meV. However, for some particular cluster configurations the excitations are localized at silicon sites directly adjacent to embedded oxygen atoms and this results in a considerable reduction of the emission energy down to approximately 1.40–1.60 eV and in an increase of the Stokes shift values to 600–800 meV. The same behavior was traced out for the case where the presence of a silanone (Si=O) bond at the surface of the $Si_{30}H_{38}O$ cluster is considered. For intermediate and high oxygen content ($i>4$) structures, a wide spread of the optical transition energies ranging from 1.60 to 3.00 eV is observed, due to the competition between two opposite tendencies. According to the first one, connected with the increasing of the quantum confinement effects due to oxidation, the optical transition energies tend to increase, whereas the enhanced possibility of involvement of oxygen or oxygen-adjacent silicon atoms in the process tends to decrease the energy transitions.

DOI: 10.1103/PhysRevB.65.195317 PACS number(s): 73.22.−f, 78.67.Hc

I. INTRODUCTION

For almost ten years, since the first experimental work[1] in the early 1990's, various silicon nanostructures have attracted a great deal of interest due to their promising optical properties as compared to the bulk material. There is a certain progress in understanding the nature of this phenomenon.[2] But the detailed mechanism of efficient visible room-temperature luminescence from such systems is still under debate.[2,3] From the theoretical point of view mainly idealized silicon nanostructures usually passivated only with hydrogen were considered,[4–11] the computational techniques used range from tight binding calculations[4] to Hartree-Fock schemes,[5,8] to semiempirical pseudopotential methods,[7] from the density functional theory within the local density approximation[6] to different approaches that try to go beyond the usual local density approximation in order to solve the well-known underestimation of the band gap.[9–11] All these works focus primarily on the size dependence of the absorption gap of hydrogenated Si clusters, mainly considering spherical clusters. Generally, the calculated quasiparticle band gaps[9,10] are larger than those computed within local density[6] and the semiempirical calculations.[4,7] Concerning the excited state properties all the results based on the Hartree-Fock method including configuration interaction,[8] on the Bethe-Salpeter technique[10] and on the time dependent local density approximation[11] show the importance of the electron-hole interaction. The calculated time-dependent local density optical gaps[11] are intermediate between the Bethe-Salpeter[10] and the Hartree-Fock ones.[8] However, for realistic silicon nanostructures, oxygen and various SiO_x phases at the surface and subsurface regions could have serious influence on the optical properties of silicon nanocrystallites.

Only a few attempts have been made to consider these effects.[5,12,13] In particular, a possible gap reduction with increasing oxygen content was first marked by Kumar *et al.*[5] However, the authors mainly investigated oxygen surface termination effects on the cluster properties and they totally excluded any processes connected with the absorption and the emission inside the cluster volume. Other interesting models have recently been proposed[8,13] for the observed shift between absorption and luminescence in silicon nanostructures. The first calculation shows that Si dots in their excited states relax to highly distorted equilibrium configurations, giving rise to new transitions involving localized states that lower the emission threshold with respect to the absorption;[8] in the second case a considerable reduction of the emission energy was predicted due to a trapped exciton at a silanone (Si=O) bond.[13] It is clear that accurate quantitative simulations and detailed study, first of all, of the excitation processes in the systems under consideration are of vital necessity for a complete understanding of the efficient luminescence process in silicon nanostructures. In particular,

the role of oxygen has to be investigated owing, also, to the very recent observation of optical gain in silicon nanoparticles embedded in silicon oxide.[14]

In this paper we perform a systematic analysis of the ground and excited states of small silicon clusters. Our aim is to trace the peculiarities of the excitations as well as the oxygen content influence on the optical transition energies. We paid special attention to the structure reorganization under such excitations and on the excitation localization.

II. COMPUTATIONAL METHOD AND CLUSTER STRUCTURE

For the cluster geometry optimization and the electronic property calculations we used the modified neglect of diatomic overlap—parametric method 3 (MNDO-PM3) in the restricted Hartree-Fock approximation in its standard parametrization.[15] This semiempirical approach is known to reproduce, on the one hand, quite correctly the geometry of small molecules and clusters as compared to the *ab initio* LCAO calculations.[15,16] And, on the other hand, it incorporates correlation effects (the parametrization was developed to properly reproduce the experimental energies of small molecules) that become very important when the size of the system is decreased. Therefore, the reflected quantitative tendencies in the energy-gap scale are essentially reliable. Considering only valence electrons and assuming the inner-shell ones to be a core together with nucleus, the electron-electron, core-core, and core-electron interactions are empirically estimated within the method. For the excited state calculations, the configuration interaction was applied.[17]

The MNDO-PM3 technique defines the values of the most probable transitions in the optical spectra as the energy difference between the lowest excited electron state (the first excited singlet state) and the ground electron state (the lowest singlet state). The transition between these two states is optically allowed and keeps the spin state stable. The absorption transition peak ($E'_{\mathrm{ex}}-E_{\mathrm{g.s.}}$ in Fig. 1) occurs when the system corresponds to the atomic configuration of the relaxed ground state. Being adiabatic, this transition does not change the structure of the cluster at the moment of excitation. However, as an electron has been transferred from a bonding like state to an antibonding one the cluster tends to relax. From this relaxed excited state an emission transition peak ($E_{\mathrm{ex}}-E_{\mathrm{g.s.}}$ in Fig. 1) appears in the optical spectra of the system. The redshift of the emission with respect to the corresponding absorption defines the Stokes shift ($E'_{\mathrm{ex}}-E_{\mathrm{ex}}$ in Fig. 1).

The procedure of geometry optimization of both ground and excited states of the cluster includes the full gradient optimization of the total energy depending on the coordinates of the atoms. For the ground state optimization we allowed all the atoms entering the system under consideration free movement. The accuracy of the calculation, i.e., the maximum gradient norm, was chosen to be not greater than 0.01 K Cal/Å. But within this parametrization, accounting for the high accuracy of the calculations, the relaxed excited state configuration cannot be obtained for all desirable structures with the same completely free movement conditions.

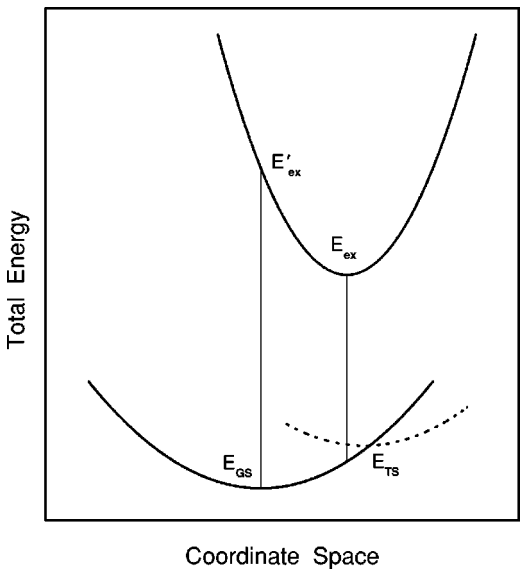

FIG. 1. Schematic diagram of the total energy in the coordinate space. (See description in the text.)

For instance, for spherical silicon clusters passivated with hydrogen with the diameter of >1 nm, we found that there existed only a local minimum at the total energy hypersurface around the excitation localized in the inner silicon layers of the clusters. The gradient norm at the minimum was from 3.5 to 8.5 K Cal/Å depending on the size and symmetry of the spherical clusters. If one goes further with the optimization procedure, in principle, it is possible to find the global minimum for the spherical cluster excited state geometry within MNDO-PM3. But, it does not correspond to the ''true'' excited state of the system. This minimum is located not so far in energy from the ground state with the heat of formation being between 5 to 30 K Cal above the ground state one and, usually, it corresponds to some kind of transitional state geometry, i.e., to the case of starting of various dynamical processes such as diffusion. If one goes back down to the ground state from such an excited state geometry, then one gets some new ground state in a point that is not stationary with considerable reconstruction of the initial ground state geometry (E_{TS} in Fig. 1). To avoid these effects some additional ''boundary'' conditions for the cluster structure should be included in the excited state geometry optimization procedure. As an example, as mentioned above in Ref. 5 only a small part of atoms, namely, those in the first surface layer, were allowed to move, whereas all the atoms in the bulk of the cluster were fixed in their initial idealized positions.

In our study we consider pyramidal shape silicon clusters (with variable oxygen content) oriented in their vertical direction along the $\langle 111\rangle$ axis of the bulk silicon [Fig. 2(a)]. To remove the dangling-bond states from the band-gap region, all the silicon dangling bonds at the surface are passivated with hydrogen. In our pyramidal cluster, made up of 30 silicon and 40 hydrogen atoms, the height is 0.943 nm and the edge length is 1.154 nm.

The reason why we choose pyramidal clusters is that, whereas several investigation have been performed for

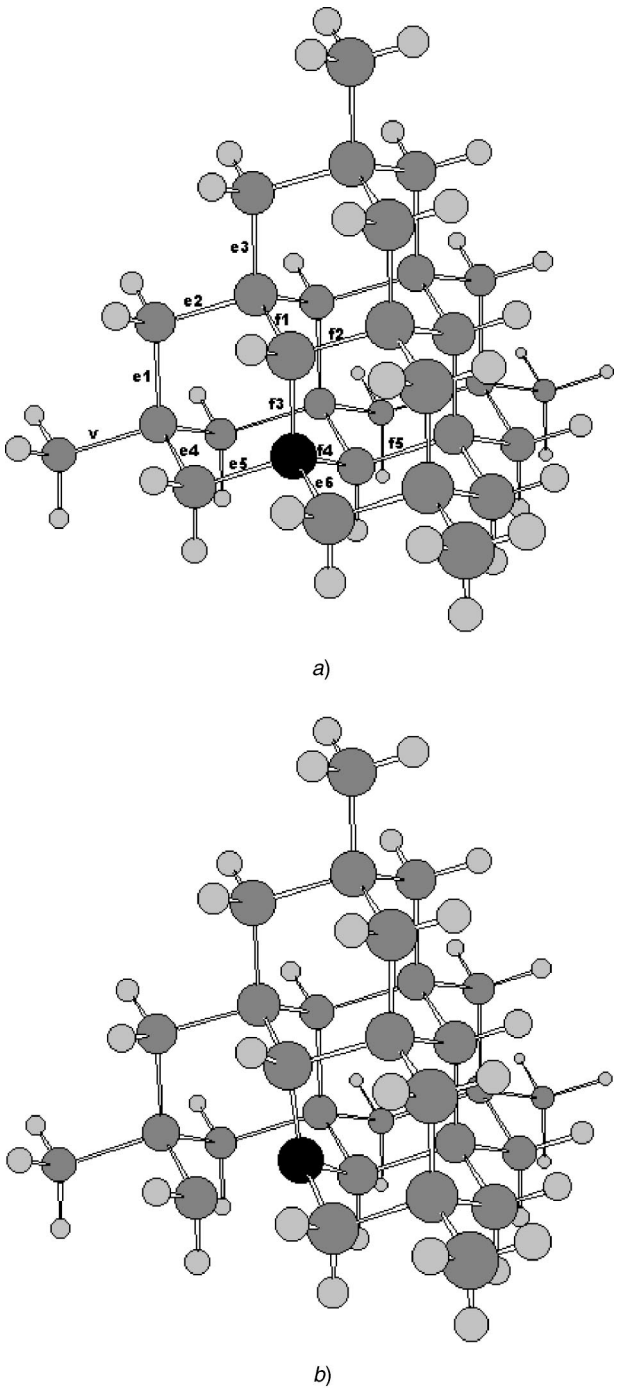

FIG. 2. $Si_{30}H_{40}$ cluster structure for the ground (a) and excited (b) states. Some of the Si-Si bonds with the possible oxygen embedding are marked with the corresponding letters denoting v (vertex), e (edge), and f (facet) followed by numbers. The silicon site underwent the maximum shift from its equilibrium ground state position is marked in black.

spherical clusters, there is a lack in the case of the pyramidal ones. In addition, these clusters can indeed represent realistic silicon nanostructures. (i) The Si nanostructures in porous silicon show a preferential faceting with respect to the (111) surfaces. (ii) Si/CaF_2 nanostructures in the form of nanocrystalline multilayers[18] or Si dots embedded in the CaF_2 matrix[19] exhibit efficient room temperature luminescence. In both structures where Si grains are presented, they show sizes in the nanometric range and are oriented preferentially along the $\langle 111 \rangle$ direction due to the epitaxial relations that exist with the low-energy $\{111\}CaF_2$ facets. (iii) Pyramidal silicon nanocrystals have recently been selectively grown on Si(001) windows in ultrathin SiO_2.[20] Moreover, as pointed out above, to calculate the relaxed excited state geometry some additional boundary conditions should be included. In our case, we assume that for the excited state geometry optimization the silicon atoms on two facets of the pyramid terminated by hydrogen [16 silicon atoms belonged to the bottom facet and the one which is opposite to the v vertex in Fig. 2(a)] are fixed in their relaxed ground state positions. This choice also corresponds to possible realistic situations. The cluster could be either the fragment of the Si/CaF_2 superlattice locked at one facet by the CaF_2 layer and at another by the similar silicon cluster, or it can represent a small silicon cluster in porous material attached to some other similar blocks in a whole wire-type structure.

III. RESULTS AND DISCUSSION

The first structure we consider is the oxygenless $Si_{30}H_{40}$ cluster. In the relaxed ground state configuration the bond lengths vary a little with the more stretched bonds of 0.238 nm at the vertex silicon atoms and going down to the value of 0.235 nm for the inner silicon atoms. The Si-H bond lengths are about 0.149 nm. The main difference in the relaxed excited state geometry as compared to the ground state one is the significant shift of one of the inner silicon atoms (marked in black in Fig. 2) from its equilibrium ground state position. The changes in its bond lengths to the surrounding nearest silicon atoms are of 0.017, -0.008, -0.005, and 0.003 nm. The other atoms remain in their equilibrium ground state positions. This shift can be thus characterized as a big enlargement of one of the Si-Si bonds [this bond is not represented in Fig. 2(b)]. One may identify the process as a strong localization of the excitation in the volume. Analyzing the appropriate wave functions of the highest occupied (HOMO) and lowest unoccupied (LUMO) molecular orbital eigenvalues, we conclude that, in the case of the ground state (absorption energy is equal to 2.35 eV; taking into account the different geometrical shape this value is in agreement with the calculated one within a similar method for a spherical cluster of comparable size),[8] the wave functions have a quite distributed character, i.e., the share of any silicon atom in the wave functions does not exceed 4%. The opposite happens for the unrelaxed and relaxed excited states (emission energy is equal to 2.20 eV). Some defined atoms exist where the wave functions are heavily localized; in both cases we can pick out five silicon atoms, representing a small silicon pyramid with one silicon atom at the center, whose contribution to the lowest (HOMO′) and highest (LUMO′) singly occupied molecular orbital wave functions is more than 75%. For the unrelaxed excited state geometry the atoms are located at the bonds marked in Fig. 2(b) as $e2$, $e3$, $f1$, and at the bond equivalent to $f1$ at the opposite facet. For the relaxed excited state, they are located near the mostly shifted

TABLE I. Heat of formation (HOF), difference between the excited and ground states heat of formation (ΔHOF), absorption (E_{ab}), and emission (E_{em}) energies, and Stokes (St) shift for $Si_{30}H_{40}O_i$ ($i=0,1,2,3$) clusters. The letters v (vertex), e (edge), and f (facet) with numbers correspond to the silicon-silicon bonds, as indicated in Fig. 2(a), where the oxygen atoms were embedded. The case with silanone bond between the silicon and terminating oxygen atoms (Si═O) is also presented for $Si_{30}H_{38}O_i$ ($i=1,2$) clusters.

	HOF (K Cal)	ΔHOF (K Cal)	E_{ab} (eV)	E_{em} (eV)	St (eV)
	−81.8	51.8	2.35	2.20	0.15
O1					
v	−174.6	51.8	2.37	2.25	0.12
$e1$	−171.9	51.0	2.35	2.21	0.14
$e3$	−168.9	49.6	2.28	2.15	0.13
$e5$	−168.9	50.1	2.28	2.17	0.11
$f2$	−164.3	49.0	2.26	2.12	0.14
$f3$	−164.3	49.4	2.26	2.14	0.12
Si═O	−122.8	36.8	1.82	1.60	0.22
O2					
$v,e1$	−269.7	49.5	2.34	2.15	0.19
$v,e2$	−263.4	49.6	2.28	2.15	0.13
$v,e3$	−262.2	49.4	2.26	2.15	0.11
$v,f3$	−257.1	49.1	2.27	2.13	0.14
$e1,e4$	−267.3	48.6	2.27	2.11	0.16
$e1,e2$	−266.4	50.2	2.25	2.18	0.07
$e1,e6$	−259.7	47.8	2.20	2.07	0.13
$e1,f2$	−257.2	49.2	2.28	2.13	0.15
$e1,f3$	−255.1	49.9	2.27	2.16	0.11
$e1,f5$	−254.5	48.9	2.22	2.12	0.10
$e2,f2$	−253.3	48.4	2.27	2.10	0.17
$e3,f2$	−253.1	47.0	2.17	2.04	0.13
$f3,f4$	−246.5	49.3	2.28	2.14	0.14
$f3,f5$	−245.8	43.9	2.03	1.90	0.13
$v,f2$	−257.9	41.9	1.92	1.81	0.11
$e1,e3$	−260.6	32.5	2.01	1.41	0.60
$e1,f1$	−257.2	34.0	2.31	1.48	0.83
$e2,f1$	−259.9	33.8	1.74	1.47	0.27
$e2$,Si═O	−216.9	49.7	2.25	2.16	0.09
O3					
$v,e1,e6$	−357.7	49.1	2.34	2.13	0.21
$v,e1,f3$	−352.4	50.2	2.28	2.18	0.10
$e1,e2,e3$	−360.2	48.2	2.17	2.09	0.08
$e2,e3,f2$	−346.7	45.6	2.07	1.98	0.09
$v,e1,e4$	−368.3	36.9	2.35	1.60	0.75
$v,e1,f1$	−354.6	32.6	2.25	1.41	0.84

silicon atom, which is at the center of the small pyramid and possesses more than 33% of the LUMO′ wave function weight. A certain redistribution of electron density in the excited states, as compared with the ground state one, is also present. The additional negative charge of about $0.10e$ is concentrated at the central silicon atom of the disturbed area.

We can say that there is a potential probability for any silicon atoms to be excited during the absorption of a photon, but, when the excitation has taken place, the excited electron will be rather space localized. Moreover, in the relaxed excited structure the excited electron space location can be shifted to some other part of the cluster volume.

In the next step we consider the $Si_{30}H_{40}O_i$ ($i=1,2,3$) clusters with all possible configurations of oxygen embedding, accounting for the symmetry conditions of the structure. Here we are interested in the oxygen induced changes on the optical properties. The most representative results are collected in Table I. In the relaxed ground state the Si-O bond lengths vary between 0.166 and 0.169 nm depending on the oxygen atom position. It is interesting to note that this value drops down to 0.164 nm, which is more similar to the one in silica, for the inner oxygen sites in the clusters having higher oxygen content. Some enlargement of the Si-Si and Si-H bond lengths for the atoms, which are directly adjacent

to the Si-O-Si bridge bond, is also present up to 0.239–0.242 and 0.150–0.152 nm, respectively. This enlargement can be connected with the existing redistribution of charges in the structures under consideration. Normally, the negative charge of 0.40 to 0.50*e* is accumulated at the oxygen atoms. The nearest silicon atoms have a positive charge of 0.33 to 1.04*e* depending on the number of adjacent oxygen atoms and accounting for the fact that there is also some negative charge transfer to the terminating hydrogen atoms. The charge transfer from these silicon atoms weaken their covalent bonds to other silicon atoms and results in a subsequent enlargement of the corresponding Si-Si bond lengths.

In the absolute majority of the studied structures, for the relaxed excited state geometry we obtained effects similar to those described above for the oxygenless $Si_{30}H_{40}$ cluster, i.e., a significant shift of one of the silicon atoms from its equilibrium ground state position. The value of the maximum enlargement of the corresponding disturbed Si-Si bond lengths is in the range of 0.008 to 0.020 nm, i.e., 3 to 8% of the standard Si-Si bond length. It is also worthwhile to note that for some particular clusters the regions of localization for the absorption and emission can coincide. This means that in these cases the absorption and emission are localized at the same silicon sites.

As one can see from Table I (ΔHOF values), the absolute majority of the cases have much in common with the simple $Si_{30}H_{40}$ structure. The heat of formation difference between the ground and relaxed excited states ranges between 45 and 52 K Cal, and the Stokes shift varies between 100 and 200 meV. These values of the Stokes shift are of the order observed for various porous silicon structures.[21] It is necessary to emphasize that in these cases the absorption and emission localization takes place at silicon atoms, which are not directly adjacent to the oxygen ones. Consequently, in such clusters the oxygen atoms have a minimum influence on the absorption and emission processes and the contribution of their wave functions to the appropriate ground state HOMO and excited states LUMO′ eigenvalues is very low ($<1\%$).

The cases at the end of each part of Table I regarding the two and three oxygen atom content structures represent exceptions. These cases can be characterized by abnormally low emission energies as compared with the other structures and, hence, by strong values for the Stokes shift that can reach as much as 800 meV. The structure of one of such clusters is shown in Fig. 3. It is seen that this big difference in behavior can be explained by accounting for the fact that in these cases the silicon atoms directly adjacent to the oxygen ones undergo the maximum shift from their ground state equilibrium positions. The atom marked in black in Fig. 3 shows changes in its bond lengths to the nearest silicon atoms of 0.017, −0.008, and −0.008 nm, whereas its bond length to the oxygen atom is still unchanged. Here oxygen plays a significant role in the creation of the ground state HOMO eigenvalues. Its contribution to the wave function can be up to 5%. So, the oxygen acts in these cases similar to an impurity atom, creating levels in the band gap and, thus, reducing the HOMO-LUMO difference. The emission energy is decreased. Moreover, the directly oxygen adjacent

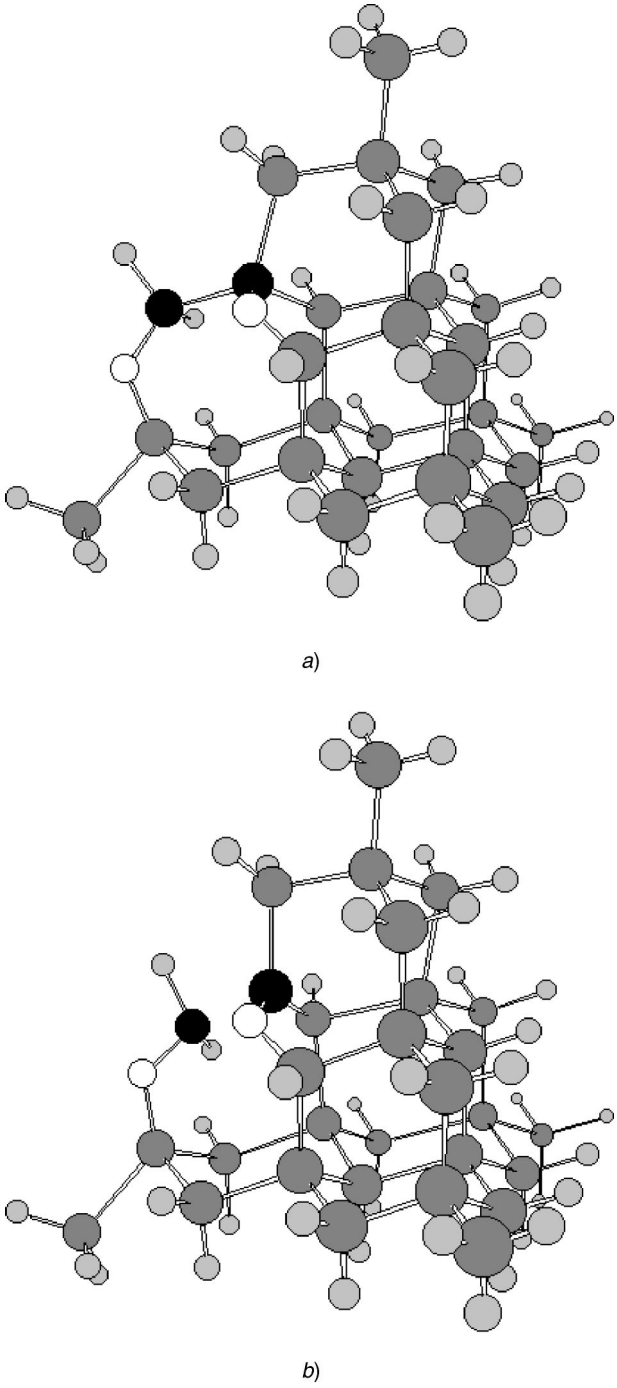

FIG. 3. $Si_{30}H_{40}O_2$ cluster structure for the ground (a) and excited (b) states. The silicon sites underwent the maximum shift from their equilibrium ground state positions are marked in black and gray.

silicon atoms, which play the main role in the formation of the excited states HOMO′ and LUMO′, have a decreased electron population in the bonding orbitals due to the electron density transfer to the oxygen sites. This results in a decrease of bonding and antibonding splitting (HOMO′-LUMO′ difference) and finally in the reduction of the excited states total energies. Thus, the conclusion is that the more the role of oxygen or adjacent silicon atoms in the

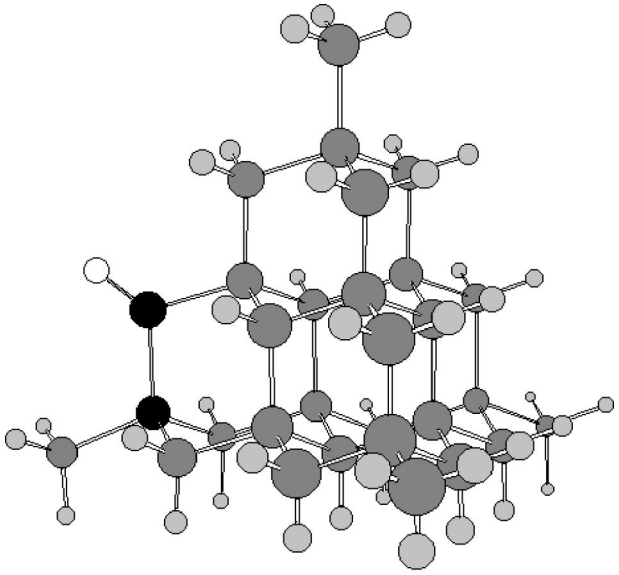

FIG. 4. $Si_{30}H_{38}O$ cluster structure for the ground (a) and excited (b) states. The silicon sites underwent the maximum shift from their equilibrium ground state positions are marked in black. The corresponding energy values are listed in Table I (Si=O line).

unrelaxed or relaxed excited state LUMO′, the more the reduction of the emission transition energy.

Another example of the exceptional cases with low values for the optical transition energies is represented by the cluster structure where a Si=O silanone bond occurs. This is shown in Fig. 4. Two hydrogen atoms passivating one of the edge silicon atoms were replaced by one oxygen atom, thus having two bonds with the silicon. In the relaxed ground state the Si=O bond length is 0.151 nm, which is considerably lower compared to the values of a normal Si-O-Si bridge bond, but corresponds well to the values obtained from *ab initio*[22] or MNDO-AM1 (Ref. 23) LCAO calculations. The other bond lengths in the system are not changed in comparison with the ground state geometry of the other one-oxygen content clusters. For the relaxed excited state the main changes in the bond length values are connected with the Si-Si bonds nearest to the silicon site having a silanone bond. One of them was increased by 0.029 nm. The other one was decreased by 0.004 nm. The two bonds, which are next to the nearest ones, just at the vertex and at the edge, were increased by 0.008 nm, whereas the Si=O bond length was shortened by about 2%. The contribution of oxygen to the ground state HOMO is now the maximum among the cases considered and is about 10%. Both the LUMO′ of the unrelaxed and relaxed excited geometries are mainly defined by the three silicon atoms nearest to the oxygen. Moreover, in the relaxed excited geometries the LUMO′ is concentrated at the two silicon atoms (more than 65%) that are connected to each other with the longest Si-Si bond. This result is in partial agreement with the conclusion in Ref. 13, thus, it partly confirms the idea about the excited electron localization around the silanone bond.

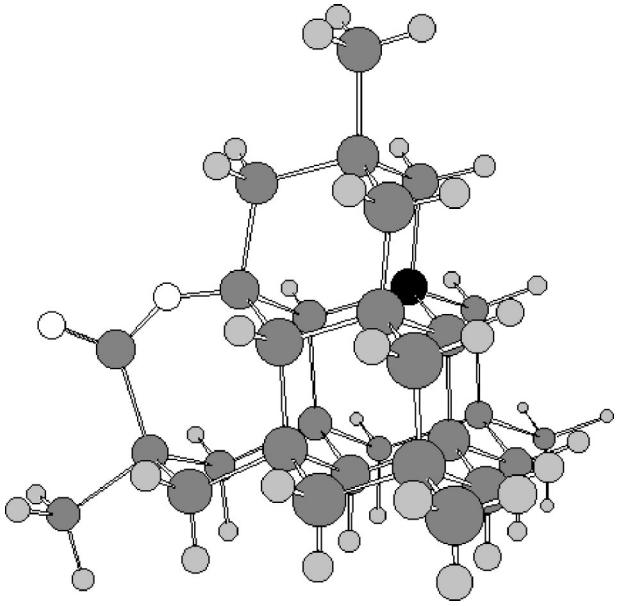

FIG. 5. $Si_{30}H_{38}O_2$ cluster structure for the ground state. The silicon site underwent the maximum shift from its equilibrium ground state position is marked in black. The corresponding energy values see in Table I ($e2$, Si=O line).

One more interesting point is that if the second oxygen atom was introduced into the structure near the Si=O with the creation of a normal Si-O-Si bridge bond (Fig. 5), the properties of the cluster change drastically. The bonds near Si=O are stabilized and the excitation occurs in the silicon matrix far from the oxygen sites (at the Si sites marked in black in Fig. 5). So, one may conclude that the silicon site at such a Si=O bond may act as a luminescent center when it is treated as a well separated interface defect center.

Experimentally, it has been reported that the luminescence of nanocrystalline Si/CaF_2 multilayers is almost size independent while the absorption is largely blueshifted when decreasing the Si layer thickness.[22,24] The Stokes shift between the optical bandgap and the luminescence peak can reach a

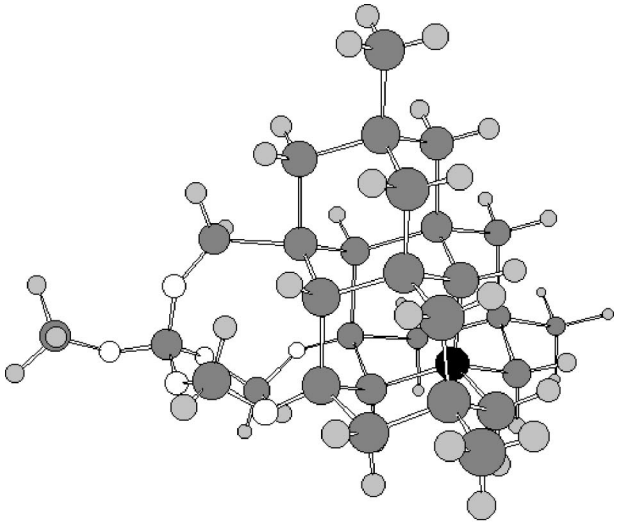

a)

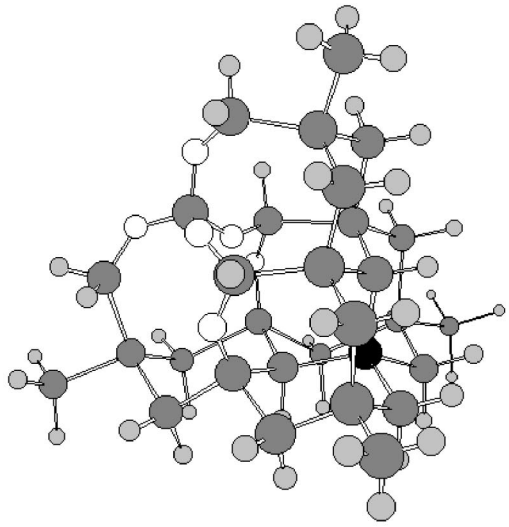

b)

FIG. 6. $Si_{30}H_{40}O_6$ ground state cluster structures for predominantly vertex (a) and edge (b) oxygen embedding. The silicon site underwent the maximum shift from its equilibrium ground state position is marked in black.

value of 1.0 eV for the thinnest Si layers, i.e., 1 nm thick. These observations were explained by deep luminescent centers located near the surface of Si nanocrystallites. This relaxation process can be related to the presence of Si=O bonds in such nanocrystalline structures.

Now we consider the cases with intermediate and high oxygen content. In the intermediate cases, i.e., with the oxygen content from four to nine oxygen atoms in the structure, we tried to trace the possible vertex as well as edge and facet oxidation processes. The examples for $i=6$ are shown in Fig. 6. Accounting for the total energies, the vertex oxidation is preferable (see Table II). The arrangement of the silicon atoms responsible for the absorption and emission can be more complex than the simple small pyramidal arrangement. For some clusters it can form a zigzag structure with four or five silicon atoms involved. But, no other special features in the energies (Table II) or the localization of the absorption and emission were observed as compared with the cases described above.

For clusters with high oxygen content we found a wide spread in the values of the optical transitions. This is due to the fact that here we have two opposite tendencies. As long as the oxygen content increases the excitation tends to be localized in the silicon matrix whose volume is decreasing, thus, the first tendency is the increasing of the confinement conditions. According to these, the energy of optical transitions rapidly increases. This is clearly demonstrated in the case of the $Si_{30}H_{40}O_{16}$ cluster example (Fig. 7), where we have well confined excited states that involve only silicon atoms (marked in black in Fig. 7). The role of oxygen in this case is negligible. That is why we found one of the highest energies of the optical transitions here (Table II). On the other hand, there is a second tendency connected with the reduction of the silicon matrix volume. This reduction gives a major probability for the oxygen atoms as well as for the oxygen adjacent silicon sites to be involved in the process creating the impuritylike levels thus reducing the HOMO′-LUMO′ difference and, therefore, decreasing the energy of the transitions. For instance, for the $Si_{30}H_{40}O_{16}$ cluster, where the 16 oxygen atoms were equally shared between the four pyramidal vertices, the emission energy is sufficiently lower. This is due to the localization of the emission in the region close to the oxygen atoms. It is also necessary to note that for some clusters, e.g., those with an oxygen content in between 20 and 32, the optimization procedure indicates that their structures are unstable, i.e., phase transition with great structure changes in the ground state becomes essential, thus they are not included in Table II.

The overall behavior of the absorption and emission energy versus oxygen content for $Si_{30}H_{40}O_i$ clusters is shown in Fig. 8. Only the most representative cases for each oxygen content in the structure accounting for the weight of the cases in the statistics were plotted in the figure. For the case of $i=16$, two values of both the absorption and emission were plotted. The higher values correspond to the case of the preferable one-vertex oxidation structure (Fig. 7), and the lower ones to the case when 16 oxygen atoms were equally shared between the four pyramidal vertices. In spite of the large spread of the values at intermediate and high oxygen content, one of the general tendencies is the certain reduction of the optical transition energies, at least for the cases of low oxygen content. This could be explained by accounting for the fact that, at earlier stages of oxidation, the effect of the increasing of the confinement conditions is negligible, whereas the oxygen atoms can still be involved in the processes, thus originating a certain reduction of the optical transition energies.

IV. CONCLUSION

The self-consistent semiempirical MNDO-PM3 method was employed to study the optical absorption and light emission in small pyramidal silicon clusters. Special attention was paid to the peculiarities of the structure relaxation and the space localization of such processes. Our main results

TABLE II. Heat of formation (HOF), difference between the excited and ground states heat of formation (ΔHOF), absorption (E_{ab}) and emission (E_{em}) energies, and Stokes (St) shift for $Si_{30}H_{40}O_i$ clusters.

i	HOF (K Cal)	ΔHOF (K Cal)	E_{ab} (eV)	E_{em} (eV)	St (eV)
4	−463.4	49.4	2.26	2.15	0.11
4[a]	−454.3	48.5	2.26	2.10	0.16
5	−566.3	48.6	2.23	2.11	0.12
5[a]	−544.7	48.9	2.27	2.12	0.15
6	−661.2	47.5	2.11	2.06	0.05
6[a]	−638.1	48.0	2.13	2.08	0.05
7	−758.3	47.1	2.14	2.04	0.10
8	−852.1	44.2	2.16	1.92	0.24
9	−956.8	46.2	2.26	2.00	0.26
12	−1259.7	41.1	1.80	1.78	0.02
14	−1462.7	36.1	1.64	1.56	0.08
16	−1685.7	56.7	2.54	2.46	0.08
16[b]	−1639.5	37.6	2.21	1.63	0.58
20	−2093.8	46.0	2.44	1.99	0.45
32	−3393.0	44.8	2.03	1.94	0.09
36	−3861.2	53.3	2.47	2.31	0.16
39	−4197.5	69.6	3.05	3.02	0.03

[a]Corresponds to the clusters with edge and facets embedded oxygen [for $i=6$ see Fig. 6(b)].
[b]Corresponds to the cluster where 16 oxygen atoms were equally shared between the four pyramid vertices.

can be summarized as follows.

In the oxygenless $Si_{30}H_{40}$ and the low oxygen-content $Si_{30}H_{40}O_i$ ($i<4$) clusters the excitations are strongly localized at the silicon sites inside the cluster volume with features which are quite similar to those in bulk silicon. So, the emission in this case can mainly be ascribed to the recombination of the simple confined exciton locked in the cluster volume. These confinement conditions result in an increased probability of the recombination process and, in turn, in an enhanced efficiency of the luminescense.

The more the oxygen content in the system under consideration, the more the influence of oxygen on the processes because of the enhanced possibility for the excitations to be localized at the silicon sites directly adjacent to embedded oxygen atoms. Here oxygen can also act as an impurity atom creating additional levels in the band gap. All of this results in a decrease of the optical transition energies. The presence of a silanone (Si=O) bond at the surface or, generally, at the interface region also considerably reduces the optical transition energies for the same reasons, i.e., due to the strong localization of the excitations at silicon sites nearest to this bond.

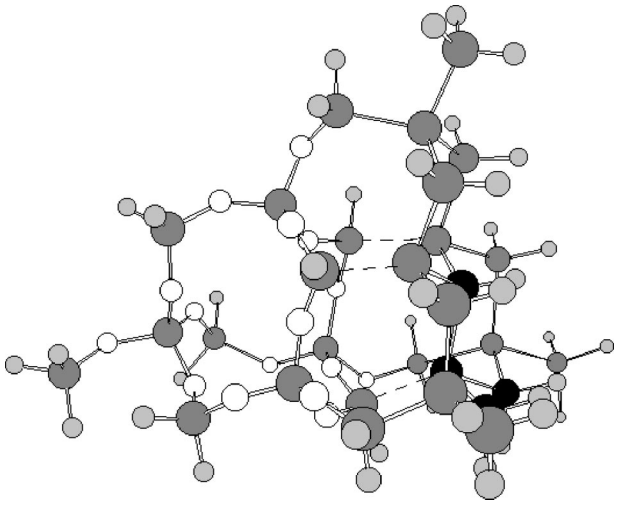

FIG. 7. $Si_{30}H_{40}O_{16}$ cluster structure for the ground state. The silicon sites underwent the maximum shift from their equilibrium ground state positions are marked by black and gray.

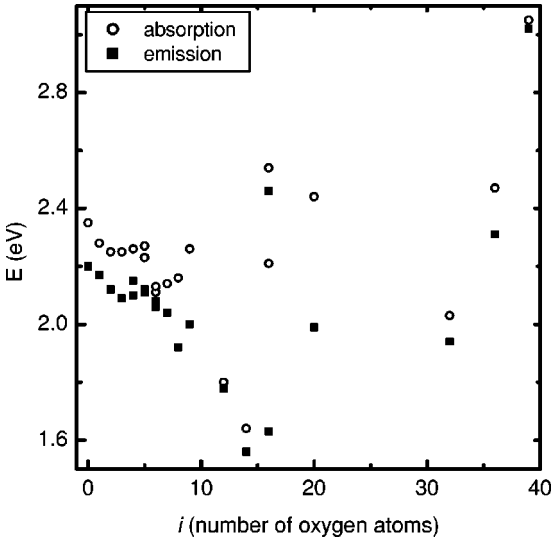

FIG. 8. Optical transition energies versus the oxygen content for $Si_{30}H_{40}O_i$ clusters.

ACKNOWLEDGMENTS

We would like to thank Dr. V. M. Zelenkovskii for helpful discussion. The authors highly appreciate the efforts of the French Ministère des Affaires Etrangères for supporting scientific cooperation between the Belarusian State University of Informatics and Radioelectronics and the Centre de Recherche sur les Mécanismes de la Croissance Cristalline. S. O. thanks INFM PRA RAMSES, MURST COFIN99, and CNRMADESSII for financial support.

[1] L. T. Canham, Appl. Phys. Lett. **57**, 1004 (1991); V. Lehmann and U. Gösele, *ibid.* **58**, 856 (1991).
[2] O. Bisi, S. Ossicini, and L. Pavesi, Surf. Sci. Rep. **38**, 1 (2000).
[3] J. P. Wilcoxon, G. A. Samara, and P. N. Provencio, Phys. Rev. B **60**, 2704 (1999).
[4] C. Delerue, G. Allan, and M. Lannoo, Phys. Rev. B **48**, 11 024 (1993).
[5] R. Kumar, Y. Kitoh, K. Shigematsu, and K. Hara, Jpn. J. Appl. Phys. **33**, 909 (1994).
[6] B. Delley and E. F. Steigmeier, Appl. Phys. Lett. **67**, 2370 (1995).
[7] A. Zunger and S. B. Zhang, Appl. Surf. Sci. **102**, 350 (1996).
[8] R. J. Baierle, M. J. Caldas, E. Molinari, and S. Ossicini, Solid State Commun. **102**, 545 (1997).
[9] S. Ogut, J. Chelikowsky, and S. G. Louie, Phys. Rev. Lett. **79**, 1770 (1997).
[10] M. Rohlfing and S. G. Louie, Phys. Rev. Lett. **80**, 3320 (1998).
[11] I. Vasiliev, S. Orgut, and J. Chelikowsky, Phys. Rev. Lett. **86**, 1813 (2001).
[12] A. M. Mazzone, Europhys. Lett. **35**, 13 (1996); A. B. Filonov, A. N. Kholod, V. E. Borisenko, A. L. Pushkarchuk, V. M. Zelenkovskii, F. Bassani, and F. Arnaud d'Avitaya, Phys. Rev. B **57**, 1394 (1998).
[13] M. V. Wolkin, J. Jorne, P. M. Fauchet, G. Allan, and C. Delerue, Phys. Rev. Lett. **82**, 197 (1999).
[14] L. Pavesi, A. Dal Negro, A. Franzó, and F. Priolo, Nature (London) **408**, 440 (2000).
[15] J. J. P. Stewart, J. Comput. Chem. **10**, 209 (1989); **10**, 221 (1989).
[16] M. J. S. Dewar and D. M. Storch, J. Am. Chem. Soc. **107**, 3898 (1985).
[17] D. R. Armstrong, R. Fortune, P. G. Perkin, and J. J. P. Stewart, J. Chem. Soc., Faraday Trans. **68**, 1839 (1972).
[18] F. Arnaud d'Avitaya, L. Vervoort, F. Bassani, S. Ossicini, A. Fasolino, and F. Bernardini, Europhys. Lett. **31**, 25 (1995); F. Bassani, L. Vervoort, I. Mihalcescu, J. C. Vial, and F. Arnaud d'Avitaya, J. Appl. Phys. **79**, 4066 (1996).
[19] F. Bassani, S. Ménard, I. Berbezier, F. Arnaud d'Avitatya, and I. Mihalcescu, Mater. Sci. Eng., B **69–70**, 340 (2000).
[20] M. Shibata, Y. Nitta, K. Fujita, and M. Ichikawa, Phys. Rev. B **61**, 7499 (2000).
[21] A. Kux and M. Ben Chorin, Phys. Rev. B **51**, 17 535 (1995).
[22] P. J. Moyer, T. L. Cloninger, J. L. Gole, and L. A. Bottomley, Phys. Rev. B **60**, 4889 (1999).
[23] M. J. Caldas, Phys. Status Solidi B **217**, 641 (2000).
[24] F. Bassani, S. Ménard, and F. Arnaud d'Avitaya, Phys. Status Solidi A **165**, 49 (1998).